Performance of the GSN station CASY-IU, 1996-2009

A report in a series documenting the status of the Global Seismographic Network

WQC Report 2010:1
January 4, 2010

Göran Ekström and Meredith Nettles

Waveform Quality Center
Lamont-Doherty Earth Observatory of Columbia University, New York

1 Station performance report: CASY

This report summarizes a number of observations that are relevant for assessing the past and current quality of the data recorded at one of the stations of the Global Seismographic Network. The purpose of the report is in part to document specific problems observed with the data. Some of these problems are related to errors in the available descriptions of station parameters: orientation of the sensors, response functions, polarities. In principle, such errors in the station metadata can be corrected by providing updated station parameters. In practice, this may be difficult in some cases due to lack of knowledge of, or inability to determine, the correct parameters. Other problems are caused by the malfunctioning of some instrument component. Regardless of the cause, it is necessary to document and publicize the lack of accurate and reliable station characteristics, especially when it is not obvious from simple inspection of the data that a problem exists.

1.1 Station CASY

The station CASY is located on the coast of Antarctica at the Australian permanent base Casey Station (see Figure 1). It is in a good location for providing global coverage in earthquake and Earth structure studies. It is in an area with very few high-quality seismic stations; the closest FDSN broadband station is DRV-G, located approximately 1500 km east of CASY.

CASY is located in an area of high seismotectonic activity in Antarctica (Figure 1). In addition, the station is within 100 km of two of the major outlet glaciers of Antarctica, one of which has also been documented as a source region for glacial earthquakes (Nettles and Ekström, 2010).

CASY is part of the USGS (IU) component of the IRIS/USGS Global Seismographic Network.

1.2 The data

Digital seismic data from CASY are available from the IRIS DMC starting in 1996. The initial installation consisted of a set of STS-1 seismometers. An auxiliary STS-2 sensor was installed in 1999. Data from CASY are included in our standard CMT analysis (Dziewonski et al., 1981; Ekström et al., 2005), and waveform data, travel-time observations, and dispersion curves derived from CASY data have been used in the development of numerous global and regional tomographic models since the station was installed.

In the analyses described here, we have made use of data collected from the IRIS DMC. We requested and downloaded all long-period (LH) and very-long-period (VH) data available at the DMC for both sensors from the start of operation (1996) until the second half of 2009. We used the currently available station metadata prepared by the Albuquerque Seismological Laboratory and available at the IRIS DMC (downloaded in December 2009). Overall, the station has been operated with few data outages since 1996.

1.3 The metadata

The dataless SEED volume for CASY documents 3 response epochs for the STS-1 (primary) and STS-2 (secondary) sensors at CASY. The STS-1 1 sps channels were initially called LHZ, LHN, LHE, without a location code. They were renamed with the location code 00 on 1999.114 (114 representing the julian day). We refer to these channels as LHZ-00, LHN-00, and LHE-00. The STS-2 sensor (location code 10) was installed in 1999 and the 1 sps channels are here referred to as LHZ-10, LHN-10, and LHE-10. The gain and frequency characteristics of the responses provided for each channel in the metadata do not indicate any changes during the period 1996–2009.

1.4 Scaling analysis

One method for assessing the quality of the data is the systematic comparison of recorded long-period waveforms with synthetic seismograms calculated for known seismic events. This analysis follows the steps described by Ekström et al. (2006). Seismic data for the LH and VH channels from both the STS-1 and STS-2 sensors are collected. Corresponding synthetic waveforms for all earthquakes in the Global CMT catalog (Dziewonski et al., 1981; Ekström et al., 2005) with $M_W \geq 6.5$ are calculated. Correlation coefficients and optimal scaling factors between observed and synthetic waveforms are calculated for the three types of data used in the standard CMT analysis: body waves (B), with periods in the range 50–150 sec, mantle waves (M), with periods in the range 125–350 sec, and surface waves (S), with periods in the range 50–150 sec. The scaling factor is only calculated for waveforms with a correlation of 0.75 or greater. The scaling factor is the number by which the synthetic seismogram should be multiplied to maximize the agreement with the observed seismogram. Annual averages of the scaling factors are calculated when four or more individual event scaling estimates are available for the year. Reversed components can be identified by their large negative correlations.

Figure 2 shows the results from our systematic comparison of CASY waveforms with synthetic seismograms. The diagrams illustrate several persistent problems with the data. For the primary (STS-1) sensor, only vertical data appear to be properly calibrated during most of the time period. The secondary (STS-2) sensor, installed in 1999, did not provide much useful data until 2003 (reflected in the lack of annual averages for the secondary sensor). The horizontal data from the STS-1 were of reversed polarity, compared with that specified in the metadata, for most of 1997 and 1998. The horizontal data from the primary sensor have been improperly calibrated since at least 1999, as reflected in the large deviations of the annual means, and the different amount of deviation in the body-wave and mantle-wave frequency bands.

1.5 Noise analysis

A second method to investigate the overall performance of the sensors is to monitor background noise levels for all seismic channels, after conversion of the data to ground acceleration. We calculate hourly rms values of the time-domain seismic signal in narrow frequency bands, and convert the rms values to a power spectral density (PSD) at that frequency using Parseval's theorem. For each month, we then calculate the low-noise value at each frequency by determining the PSD amplitude not exceeded 10% of the time.

The PSD data provide a wealth of information about the station and the sensors. Figure 3 shows the monthly low-noise estimate for each LH channel at 72 s period since 1996. The first observation is that the station has been providing data without major outages since 1996. Second, the noise data suggest that the only stable period of operation was soon after installation, during which time the LHZ, LHN, and LHE low-noise estimates exhibit stable and reasonable values. As seen in Figure 2, 1996 was the only year for which we obtained good scaling measurements (corresponding to acceptable fits to synthetic waveforms) for all three components in both the body- and mantle-wave frequency bands.

The STS-2 sensor appears to have had major problems during the period 1999-2003. The LHE-10 component has an unrealistically low noise level, while the vertical-component values are off scale in Figure 3. The lower levels of horizontal noise observed on the STS-1 components (LHN-00, LHE-00) after 1999 are erroneous, as it is clear that the response functions are incorrect for these channels (see Figure 2).

1.6 Inter-sensor coherence

An additional method to assess the quality and calibration of the recorded signals is to calculate inter-sensor coherence. This analysis is possible when more than one sensor is operated in the same location. At CASY, this is possible for the period 1999-2009, during which time both STS-1 and STS-2 instruments have been operating.

We calculate the coherence of the deconvolved vertical, N–S, and E–W components. The coherence is calculated for $\sim$2-hour-long time windows containing the signals for earthquakes with $M_W \geq 6.5$ (the same events used in the scaling analysis). For each pair of seismograms, the coherence is calculated in narrow frequency bands around 32 s, 64 s, 128 s and 256 s. If the coherence is greater than 0.95, the value is stored together with the complex scaling factor (represented here as a scaling factor and phase shift) that should be applied to the secondary-sensor data to bring the two time series into the best agreement.

Figure 4 shows the results of the coherence analysis for the vertical component. For the time period 2003–2009, there is good agreement between the two sensors, both in the amplitude and the phase at all four periods. There is an indication that the STS-1 gain may be smaller by a few percent than indicated in the metadata for the period since 2005. Alternatively, the STS-2 gain may be too large by the same amount. No time windows with coherent waveforms were found for most of the period 2000–2003, suggesting a serious problem with the STS-2 waveforms since the STS-1 waveforms match the synthetics for many events during this time period (Figure 2).

The horizontal components show very different results. Figure 5 shows the amplitude and phase differences for the N–S components. The agreement between the signals is never good during the time interval 1999–2009, with amplitude factors varying between 0.1 and 0.9 depending on the period and the time. The time variations are dramatic, showing an annual periodicity with the largest deviations in the early months of each year.

Figure 6 shows the results for the E–W component. Remarkably, the results are very similar to those of the N–S component, with the same seasonal periodicity. Since the horizontal components of the STS-2 provide good scaling to the synthetic waveforms (Figure 2), we infer that the time-dependent differences should be attributed to the STS-1. However, since the horizontal components originate from individual seismometers, it is not clear to us why the differences are so similar for the two components.

1.7 Polarization analysis

The orientation of the horizontal components can be assessed empirically by comparing observed and synthetic waveforms, and finding the angle by which the horizontal components should be rotated in order

to maximize the agreement. We follow the approach described by Ekström and Busby (2008) for such a comparison, using the observed and synthetic waveforms from Global CMT analysis.

We apply the method of Ekström and Busby (2008) to the same dataset used in the scaling analysis. Figure 7 shows the individual measurements for the period of operation for the different channels. Overall, the number of useful observations is small, a consequence of the poor quality of the horizontal data from both sensors. The median rotation angle for the STS-2 is $-7°$, and nearly all measurements in Figure 7 show deviations of the same sign, suggesting that the instrument may be misoriented. The median estimates for the entire period of operation is given in Table 1.

Comp. 1	Comp. 2	First	Last	# Obs.	N	Az 1	Az 2	25%	Med.	75%
LHE	LHN	19960221	19990405	110	5	90	0	-11	-3	-1
LHE-00	LHN-00	19990510	20041226	176	9	270	180	-10	-6	0
LHE-10	LHN-10	19990510	20041226	176	11	90	0	-12	-7	-1

Table 1: Statistics of sensor-rotation angles estimated in this study. Columns are the channel names, the dates of the first and last observation contributing to the estimate, the total number of observations, the number of observations of acceptable quality, the reported azimuths of sensitivity of the two channels, the median polarization-angle deviation from the reported orientation together with the range of the second (25%) and third (75%) quartiles of the observations.

1.8 Example seismograms

The anomalies described here agree with observations we have made in our routine analysis of waveforms for the determination of CMT earthquake parameters. When confronted with the seismograms for an individual earthquake, it is often difficult to assess whether a poor fit is due to incorrect source parameters, inadequate modeling of wave propagation through an Earth model, or some problem with the recorded seismograms. Here, we have included some examples of data that illustrate the characteristics of the types of problems that we have encountered with data from the CASY station.

Figure 8 shows examples of three-component mantle- and surface-wave data for two events recorded in 1996 and 1997 on the STS-1 seismometer. The 1996 event (top panel) occurred just days after installation of CASY, and the mantle-wave fits are good. All components are well matched, including the rotated components. This quality of fit is seen only during the first 12 months of operation of the CASY station. The bottom panel shows the observed and synthetic surface waves for an earthquake in 1997. These seismograms illustrate the polarity change of the horizontal components that appears to have occurred in early 1997, but which is not reflected in the metadata until 1999.114. The waveforms are fit well, apart from a 180-degree phase shift for the horizontal components. Note that the rotation of horizontal components into longitudinal and transverse directions appears to be close to perfect, illustrating that the sensors are well oriented.

The top panel of Figure 9 shows a comparison between seismograms recorded on the STS-1 seismometer and the corresponding synthetic waveforms for an event on February 18, 2009. Both the amplitude and the phase of the waveforms are poorly matched on the horizontal components, indicating an error in the STS-1 response function. The bottom panel of Figure 9 shows the comparison between seismograms recorded on the STS-2 seismometer and the corresponding synthetic waveforms for the same event. For this sensor the fit is good. The background noise is significantly higher for the STS-2 sensor, perhaps reflecting the location and quality of the installation, but the correlation between observed and synthetic waveforms indicates that the STS-2 sensor is operating properly and is well calibrated.

2 Summary and analysis

At the time of writing (January 2010), the GSN station CASY is performing poorly. Only the vertical component of the primary sensor is operating at, or close to, the expected quality. The proper functioning of the vertical component is supported by the observation that both body- and mantle-wave waveforms are fit well by synthetics in the CMT analysis (Figure 2). Seasonal variations in Earth noise are also resolved by the vertical STS-1 sensor (Figure 3), and noise levels have been nearly constant since 1996. The vertical STS-1 and STS-2 seismometers agree to within approximately 5% (Figure 4).

The horizontal STS-1 seismometers are malfunctioning and have been malfunctioning since at least 1998. The response is dramatically time dependent as well as frequency dependent. This is demonstrated best by the comparison with synthetic waveforms (Figure 2) and the coherence analysis (Figure 5 and Figure 6). The noise analysis is consistent with this interpretation, but is by itself not conclusive. In fact, based only on the data presented in Figure 3, one might conclude that horizontal noise levels have decreased since 1996. No useful data have been recorded by the horizontal STS-1s since 1998.

The STS-2 data appear to have been faulty between 1999 and sometime in 2003. Since 2003, the STS-2 appears to be recording ground motion properly, at least intermittently, although the noise levels (Figure 3) suggest that the installation of this instrument does not meet observatory standards, considering the high quality of data that was obtained during 1996 in the same location by the STS-1.

The STS-1 horizontal data show that the polarity of both the N–S and E–W sensors changed around 1997.001, a change not properly reflected in the metadata. No significant change is seen in the PSD analysis at that time, and Figure 2 shows that observed and synthetic waveforms remained highly coherent, although with a reversed polarity.

3 Conclusions and recommendations

This analysis shows that CASY generated data of GSN quality only for the first 12 months of operation and has suffered from chronic sensor problems since 1998, a period of more than 10 years. Unfortunately, the highly erratic behavior of the horizontal components makes it unlikely that any retroactive remedy for the observed problem will be possible. There is some suggestion that the data from 1997 are of good quality, and the only problem for that year may be that the polarities of the horizontal components are reversed.

The sensor problems identified here should have been identified early on, and corrected. We speculate that the problem went unnoticed or undiagnosed because no routine calibrations are performed at GSN stations. The lack of systematic calibrations, and inspection of calibration results, makes it difficult to identify instrument problems. In addition, the lack of calibrations makes it close to impossible to repair errors in instrument parameters once a problem has been identified. Some of the symptoms of the STS-1 malfunction are similar to those observed at other stations (Ekström et al., 2006); interpretation is complicated by the presence of multiple sensor problems.

Modern seismological analyses require well-calibrated instruments. Amplitude variations of 10% and smaller are interpreted as signals in modern studies that seek to map the attenuating properties of the Earth's interior (e.g., Dalton and Ekström, 2006). Phase anomalies of a few seconds at long periods are similarly interpreted in terms of Earth's elastic structure by numerous authors. Data from CASY have been used in such studies with the assumption that the station is meeting GSN design goals (Lay et al., 2002) with respect to instrument stability. Clearly it does not, and its failure to do so should be documented. This is particularly important when, as for CASY, the data may appear visually to be correct, but are actually faulty.

It is urgent to restore CASY to a state where it generates GSN-quality data. It is especially unfortunate that the STS-2 has not provided quality replacement data during the last 10 years. It would be fruitful to determine why the STS-2 is so noisy, and to consider a high-quality re-installation of that instrument (if it is otherwise functional) while the cause of the STS-1 malfunction is investigated and addressed.

4 References

Dalton, C. A., and G. Ekström, Global models of surface wave attenuation, *J. Geophys. Res.*, 111, B05317, 2006.

Dziewonski, A. M., T.-A. Chou, and J. H. Woodhouse, Determination of earthquake source parameters from waveform data for studies of global and regional seismicity, *J. Geophys. Res.*, 86, 2825–2853, 1981.

Ekström, G., A. M. Dziewonski, N. N. Maternovskaya, and M. Nettles, Global seismicity of 2003: Centroid-moment tensor solutions for 1087 earthquakes, *Phys. Earth Planet. Inter.*, 148, 327–351, 2005.

Ekström, G., C. A. Dalton, and M. Nettles, Observations of time-dependent errors in long-period gain at global seismic stations, *Seism. Res. Lett.*, 77, 12–22, 2006.

Ekström, G., and R. W. Busby, Measurements of seismometer orientation at USArray Transportable and Backbone stations, *Seism. Res. Lett.*, 79, 554-561, 2008.

Lay, T., J. Berger, R. Buland, R. Butler, G. Ekström, B. Hutt, B. Romanowicz, *Global seismic network design goals update 2002*, IRIS GSN committee report, 2002.

Nettles, M., and G. Ekström, Glacial earthquakes in Greenland and Antarctica, *Annual Reviews*, in review, 2010.

Peterson, J., Observations and modeling of background seismic noise, *U. S. Geol. Surv. Open-file Rep. 93-322*, 1–45, 1993.

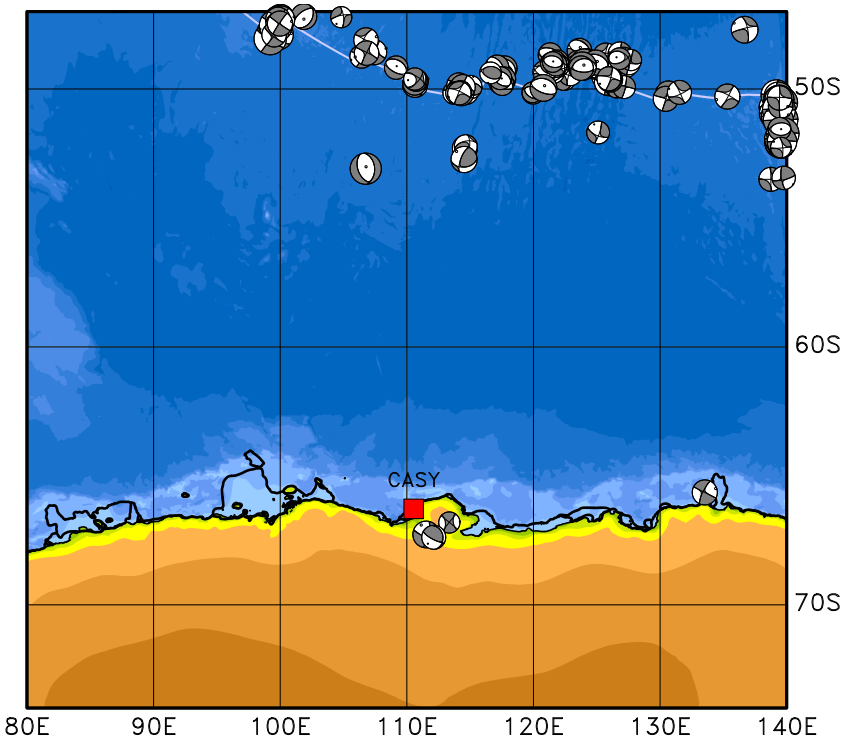

Figure 1: Map showing the location of CASY (red square) on the coast of Antarctica. Grey focal mechanisms show locations and moment tensors of earthquakes in the Global CMT catalog. The earthquakes to the North are associated with the ridge-transform boundary between Australia and Antarctica. The three focal mechanisms near CASY are representative of a class of rare intraplate continental earthquakes occurring along the coast of Antarctica. No other FDSN or GSN station is located within the boundaries of the map.

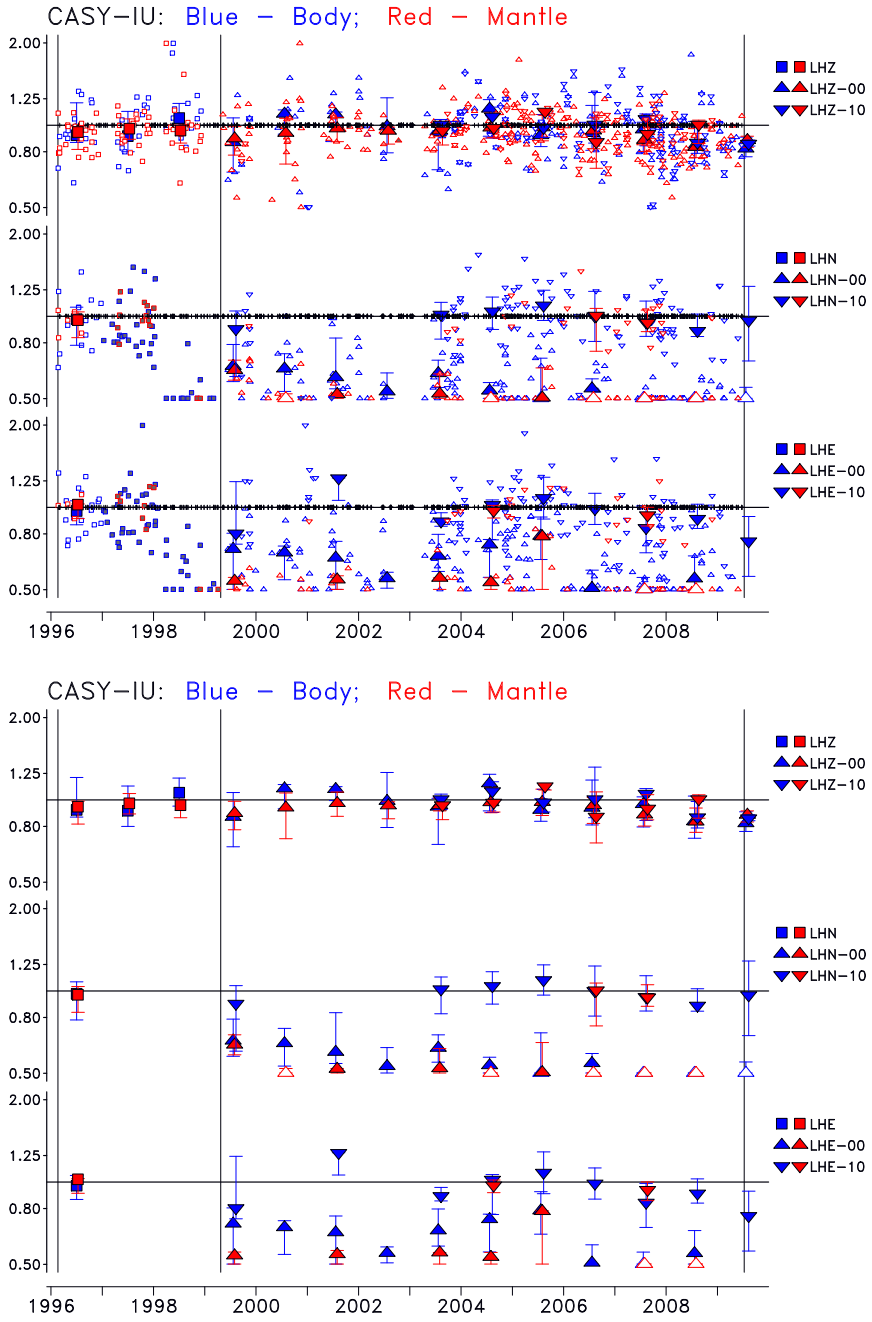

Figure 2: Scaling factors for the different data channels at CASY. Small symbols in top panel show scaling factors for individual traces. Tic marks on the horizontal axes show times of observations for which the correlation was less than 0.75. Large symbols show the median scaling factor for each year, with the error bars corresponding to the range of the second and third quartiles of the scaling factors. The legend on the right identifies the symbol type with a specific channel. Large open symbols indicate that the annual scaling factor was smaller than 0.5. Small filled symbols indicate individual traces with good correlation but reversed polarity. Thin vertical lines show the response epoch boundaries present in the metadata (1996.050, 1999.114 and 2009.191). Bottom panel shows only the annual median values.

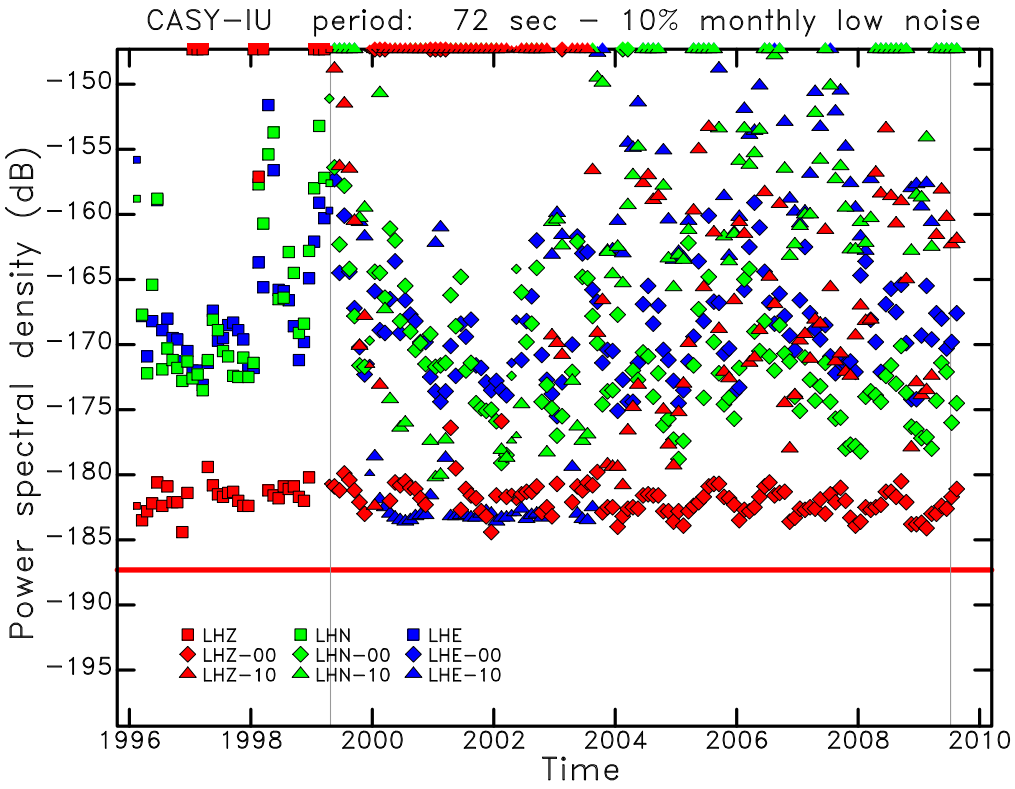

Figure 3: Diagram shows the monthly PSD of ground acceleration at 72-s period for all long-period (LH) channels at CASY for the period 1996–2009. Smaller symbols are used for months with fewer available hourly measurements. Off-scale measurements are plotted at the edges of the diagram. Each component and sensor is represented by a distinct symbol and color. The red horizontal line indicates the level of Peterson's (1993) Low Noise Model (LNM) at 72 s. The thin vertical lines show the times of epoch boundaries in the station metadata.

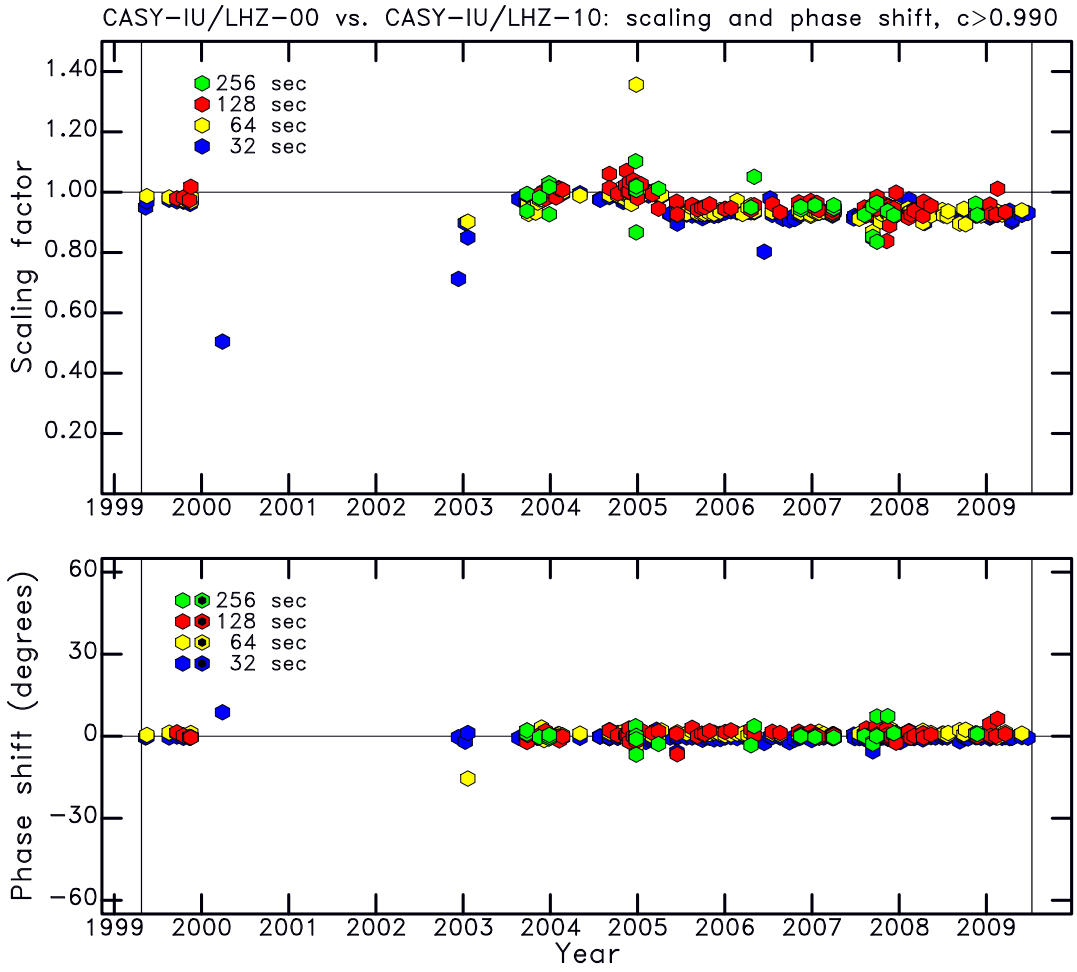

Figure 4: Diagram shows the result of coherence analysis for the vertical component of the STS-1 and STS-2 sensors. Each symbol represents a measurement of coherence for an $M_W \geq 6.5$ earthquake. The minimum coherence plotted is indicated by c. The scaling and phase shift between the two time series is shown at four different periods. The scaling factor is close to 1.0 and the phase angle is 0, indicating that the sensors have consistent gain and frequency-response information. The scaling value is around 0.95 for the most recent time period (since 2005), indicating that the overall STS-1 gain may be $\sim$5% less than the value provided in the metadata. The thin vertical lines show the times of epoch boundaries in the station metadata.

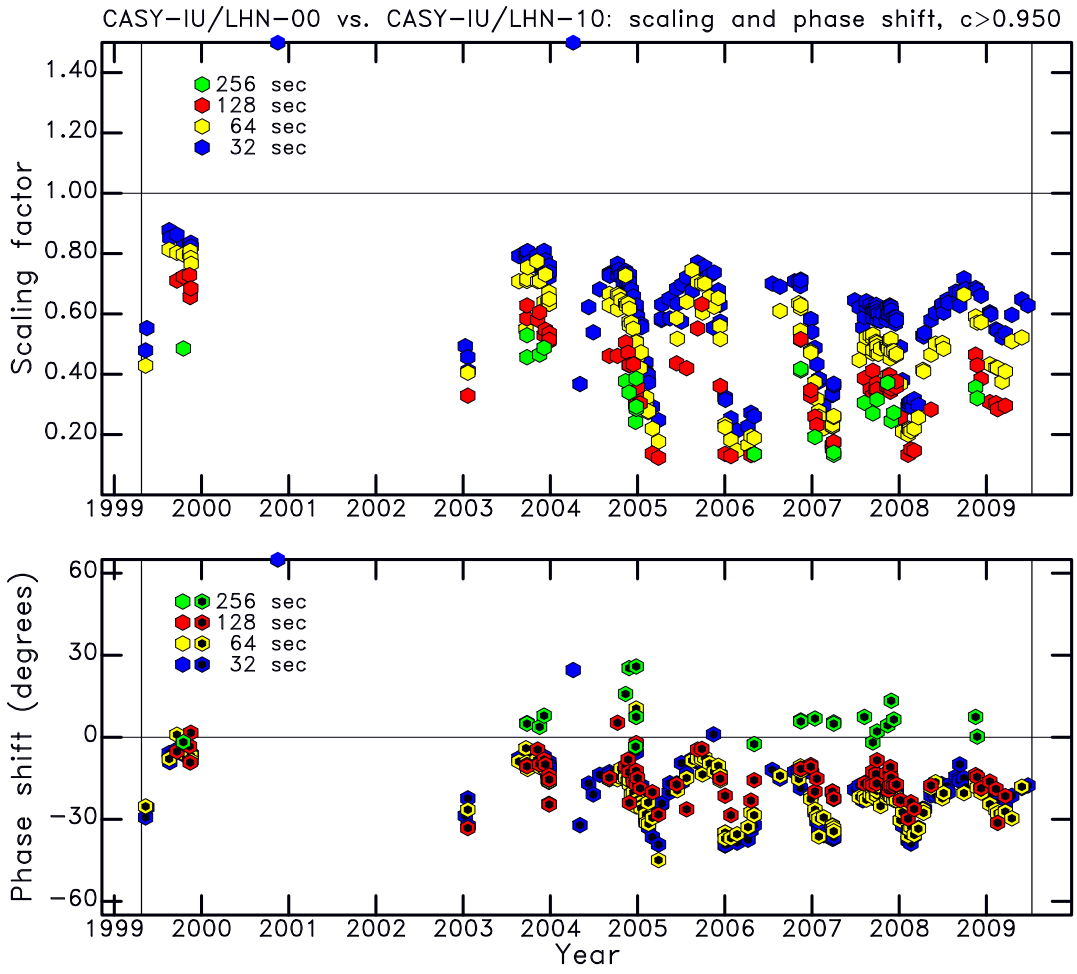

Figure 5: Same as Figure 4, but for the North-South components. A black dot in the symbol indicates that the phase shift is in addition to a 180-degree phase shift. This is consistent with the fact that the STS-1 horizontal seismometers are reversed in orientation with respect to the STS-2 (the orientations are correctly represented in the metadata for this epoch). Large, frequency-dependent and time-varying differences in the amplitude and the phase between the signals is seen during the entire time period. The variations have a clear seasonality, with the largest deviations during the austral summer.

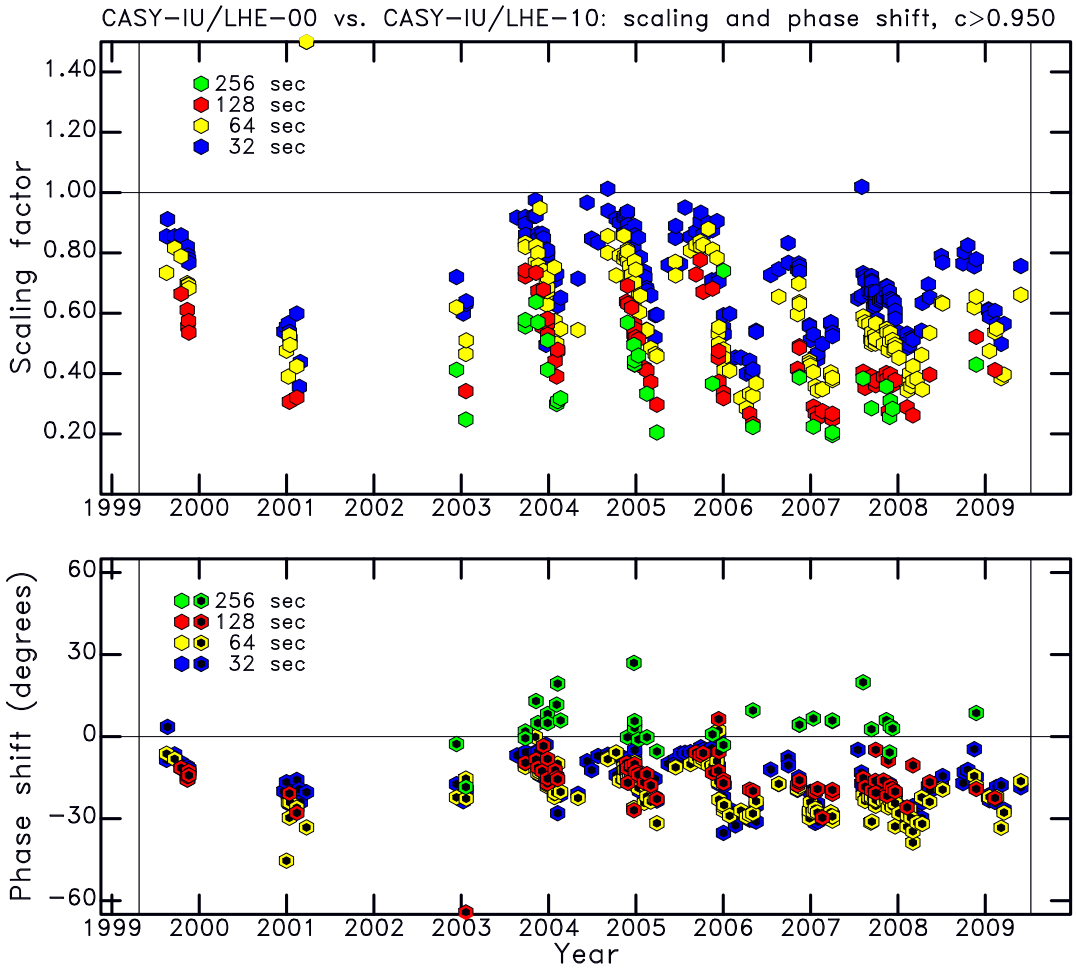

Figure 6: Same as Figure 5, but for the East–West components.

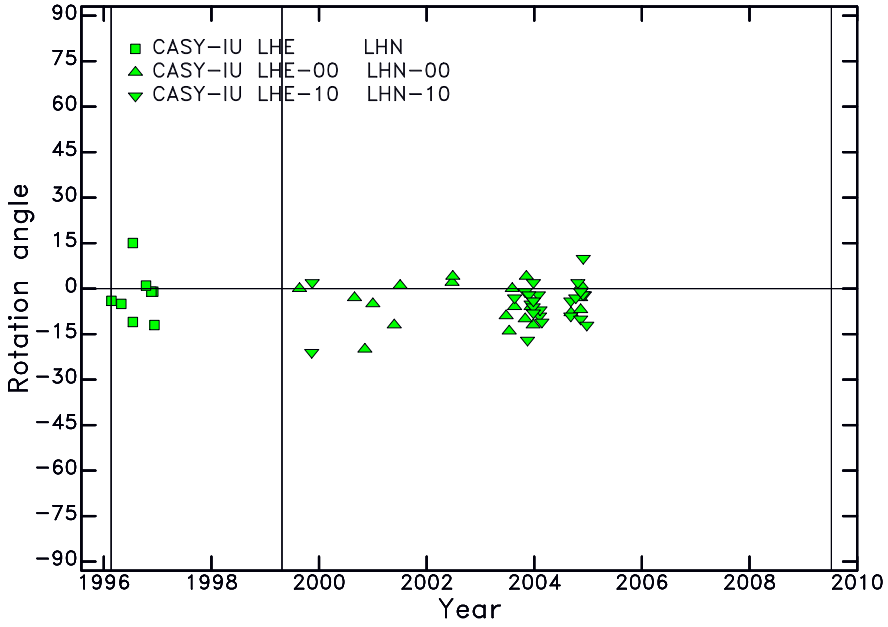

Figure 7: Individual measurements of polarization angle as a function of time. All measurements for the period of operation are shown. Symbols represent measurements obtained in the surface-wave band of the CMT analysis. The thin vertical lines show the times of epoch boundaries in the station metadata.

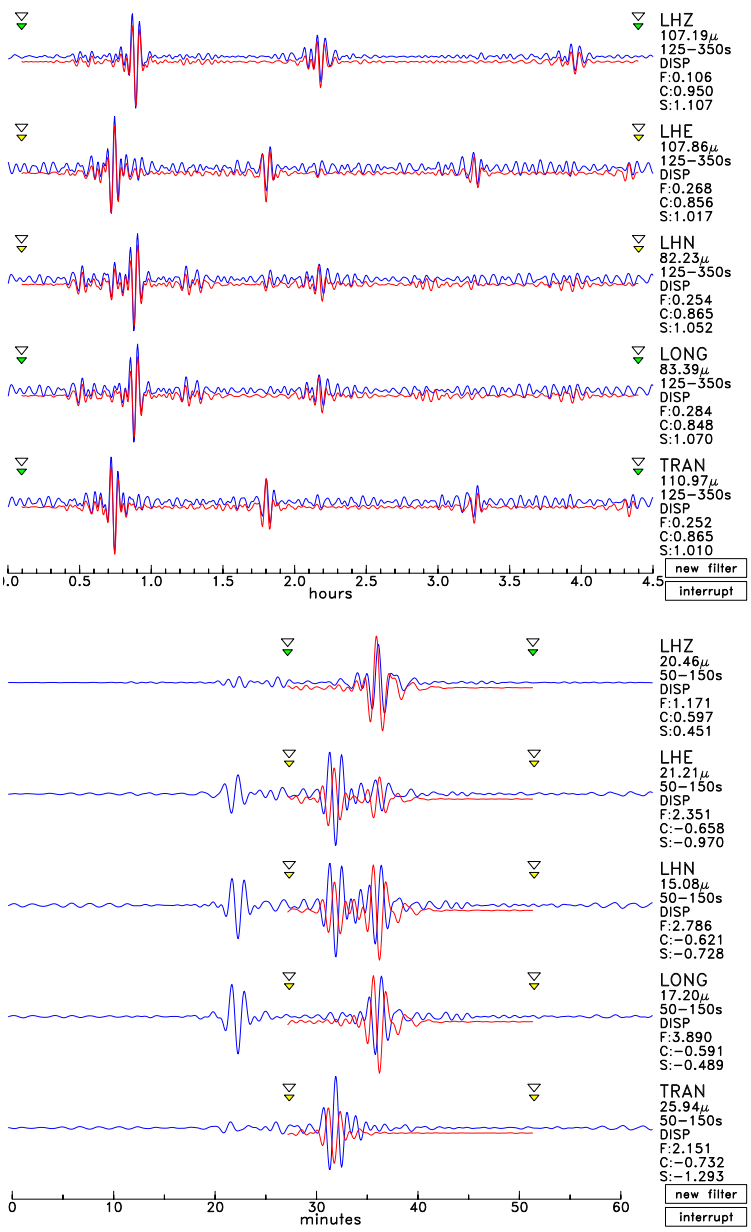

Figure 8: (Top) Comparison of observed (blue traces) and synthetic (red traces) mantle-wave seismograms for an M_W = 7.5 earthquake on February 21, 1996. The good fit indicates that the instrument was operating well soon after installation. The channel name, maximum displacement, and values for the three parameters residual misfit (F), correlation (C) and scaling factor (S) are given to the right of each waveform. (Bottom) Observed and synthetic surface-wave seismograms for an earthquake on June 10, 1997. The horizontal components are reversed in polarity.

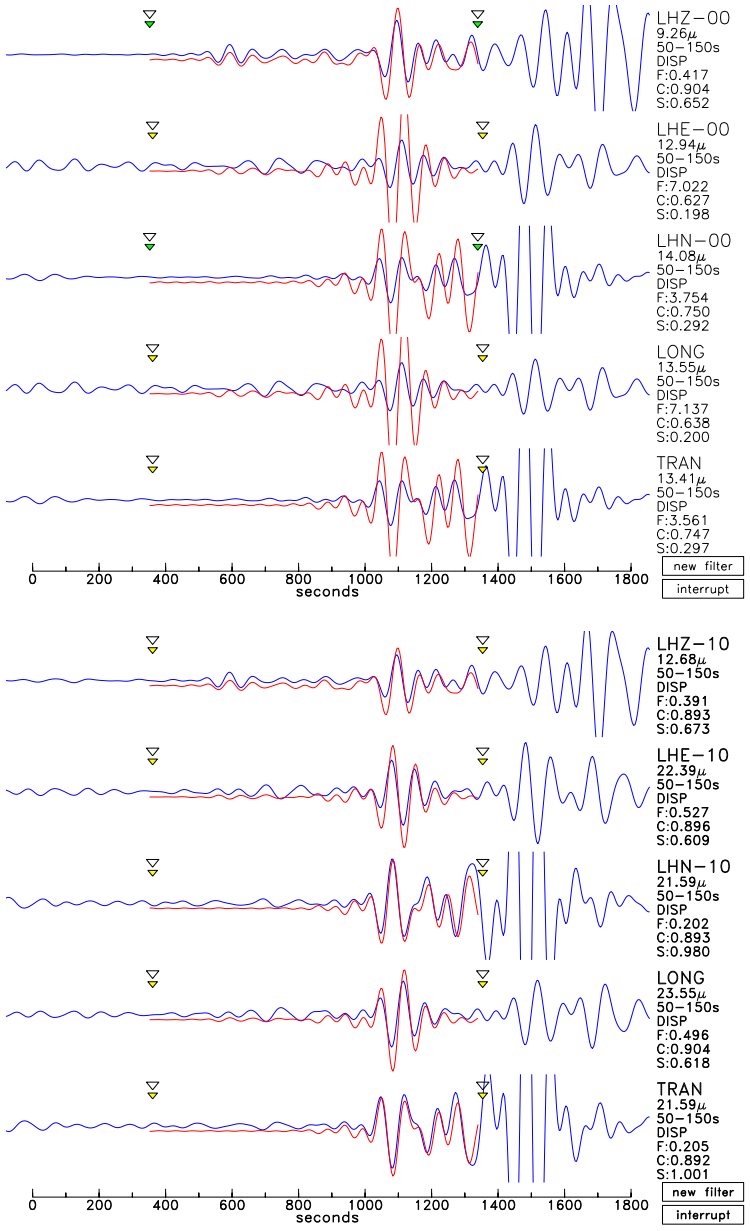

Figure 9: (Top) Observed (STS-1) and synthetic body-wave seismograms for an earthquake on February 18, 2009. The fit is characteristic of the problem that has existed at CASY since 1999. Horizontal body waves are poorly fit. The problem is not only a difference in gain. The fit for the vertical component is adequate. (Bottom) Observed (STS-2) and synthetic body-wave seismograms for the same earthquake, but recorded on the STS-2 seismometer. The fit to all three components is adequate. The noise level on the STS-2 seismometer is higher than on the STS-1 seismometer, but the agreement between the observed and synthetic waveforms indicates that the STS-2 seismometer is functioning properly and is correctly calibrated.